PCCP

ROYAL SOCIETY OF CHEMISTRY

PAPER

View Article Online
View Journal | View Issue

Check for updates

Cite this: *Phys. Chem. Chem. Phys.*, 2022, **24**, 26458

A new route for enantio-sensitive structure determination by photoelectron scattering on molecules in the gas phase

Kilian Fehre,*[a] Nikolay M. Novikovskiy,[bc] Sven Grundmann,[a] Gregor Kastirke,[a] Sebastian Eckart,[a] Florian Trinter,[ad] Jonas Rist,[a] Alexander Hartung,[a] Daniel Trabert,[a] Christian Janke,[a] Martin Pitzer,[a] Stefan Zeller,[a] Florian Wiegandt,[a] Miriam Weller,[a] Max Kircher,[a] Giammarco Nalin,[a] Max Hofmann,[a] Lothar Ph. H. Schmidt,[a] André Knie,[b] Andreas Hans,[b] Ltaief Ben Ltaief,[b] Arno Ehresmann,[b] Robert Berger,[e] Hironobu Fukuzawa,[f] Kiyoshi Ueda,[f] Horst Schmidt-Böcking,[a] Joshua B. Williams,[g] Till Jahnke,[h] Reinhard Dörner,[a] Philipp V. Demekhin*[b] and Markus S. Schöffler*[a]

Received 7th July 2022,
Accepted 15th September 2022

DOI: 10.1039/d2cp03090j

rsc.li/pccp

X-Ray as well as electron diffraction are powerful tools for structure determination of molecules. Studies on randomly oriented molecules in the gas phase address cases in which molecular crystals cannot be generated or the interaction-free molecular structure is to be addressed. Such studies usually yield partial geometrical information, such as interatomic distances. Here, we present a complementary approach, which allows obtaining insight into the structure, handedness, and even detailed geometrical features of molecules in the gas phase. Our approach combines Coulomb explosion imaging, the information that is encoded in the molecular-frame diffraction pattern of core–shell photoelectrons and *ab initio* computations. Using a loop-like analysis scheme, we are able to deduce specific molecular coordinates with sensitivity even to the handedness of chiral molecules and the positions of individual atoms, *e.g.*, protons.

Open Access Article. Published on 28 Okitobba 2022. Downloaded on 07/10/2025 03:30:00.
This article is licensed under a Creative Commons Attribution 3.0 Unported Licence.

Introduction

During the last decade, the determination of the three-dimensional structure of molecules using electron crystallography developed into a complementary analysis method to the well-established X-ray crystallography.[1–3] In particular, for the structural investigation of micro- and nano-crystalline materials, where sufficiently large single crystals for X-ray diffraction cannot be obtained[4] or crystalline-sponge approaches for X-ray diffraction[5,6] fail, electron diffraction is the method of choice.[7] It yields Ångstrom resolution even when applied to large systems[8] or systems involving weak scatterers such as hydrogen atoms.[9] For cases in which molecular crystals cannot be obtained or the interaction-free molecular structure is to be addressed, corresponding electron-scattering approaches on gas-phase molecules exist.[10,11] Such electron diffraction studies on randomly oriented molecules, however, can only provide information on interatomic distances, which is, in addition, challenging to extract in case of overlapping distance parameters. Furthermore, they do not reveal the handedness of chiral systems.[12] In order to overcome the drawback of a random orientation of the molecules under investigation, several experiments have been performed utilizing electron[13,14] and X-ray diffraction[15] in combination with sophisticated two-dimensional and three-dimensional laser-alignment schemes.

An alternative approach employs electrons that are created from within the molecule as a probe. In these experiments, highly energetic single photons or strong-field laser pulses ionize isolated molecules in the gas phase. The emitted photoelectron is scattered by the molecular potential, yielding a very complex interference pattern, in which the structural

[a] *Institut für Kernphysik, Goethe-Universität Frankfurt, Max-von-Laue-Straße 1, 60438, Frankfurt am Main, Germany. E-mail: fehre@atom.uni-frankfurt.de, schoeffler@atom.uni-frankfurt.de*
[b] *Institut für Physik und CINSaT, Universität Kassel, Heinrich-Plett-Straße 40, 34132, Kassel, Germany. E-mail: demekhin@physik.uni-kassel.de*
[c] *Institute of Physics, Southern Federal University, 344090, Rostov-on-Don, Russia*
[d] *Molecular Physics, Fritz-Haber-Institut der Max-Planck-Gesellschaft, Faradayweg 4-6, 14195, Berlin, Germany*
[e] *Department of Chemistry, Philipps-Universität Marburg, Hans-Meerwein-Straße 4, 35032, Marburg, Germany*
[f] *Institute of Multidisciplinary Research for Advanced Materials, Tohoku University, Sendai, 980-8577, Japan*
[g] *Department of Physics, University of Nevada, Reno, Nevada, 89557, USA*
[h] *European XFEL GmbH, Holzkoppel 4, 22869, Schenefeld, Germany*

This journal is © the Owner Societies 2022

Open Access Article. Published on 28 Okitobba 2022. Downloaded on 07/10/2025 03:30:00.
This article is licensed under a Creative Commons Attribution 3.0 Unported Licence.

information is encoded. Using table-top laser systems, laser-induced electron diffraction (LIED) has, for example, proven its capability determining internuclear distances with high accuracy for small molecules.[16–18] In general, photoelectron diffraction by molecules in the gas phase has been successfully applied for determining molecular constituents,[19] mapping bond lengths[20,21] and simple chemical reactions[22] on ultrafast timescales.[17] Until now, however, corresponding studies were restricted to linear[17,19,22] or mostly symmetric molecules[23–25] such as, *e.g.*, CO, CO_2, H_2O, or CH_4.

Apart from measuring the electron-diffraction pattern (in terms of an electron angular emission distribution), the key to electron diffraction experiments on molecules is the knowledge of each individual molecule's orientation in space.[26] A possible approach is to adsorb the molecule to a surface[13] or (as indicated above) to utilize weak laser pulses in various schemes (and in 2D or 3D arrangements) to orient[27,28] or align[15,27–31] the molecule. Single-cycle pulses in the THz were also used in the past to orient/align molecules.[32] An alternative approach for detecting the molecule's spatial orientation is Coulomb explosion imaging,[33] which, in addition, provides structural information, as well. Here, molecular ions or molecules are rapidly charged up by foil-induced electron stripping,[33] multiple ionization by a short and strong laser pulse, or by photoionization and subsequent Auger decay (cascades).[34] After the charge-up, the ionic fragments are driven apart rapidly by Coulomb repulsion. Intriguingly, if more than three molecular fragments are generated in the Coulomb explosion, the triple product of three of their momentum vectors allows for identifying whether a chiral molecule was right- or left-handed.[35] However, despite the absolute configuration of chiral molecules can be determined in principle using this method,[35,36] it has been restricted, so far, to small molecules with only a few atoms. So far, the largest molecule investigated using this approach was halothane consisting of eight atoms,[37] but just recently iodopyridine (11 atoms) has been addressed in an experiment.[38] Seribal *et al.* have shown in a simulation that Coulomb explosion imaging in combination with a spatial orientation of the gas-phase target substance allows for retrieving the molecules' handedness even for systems as large as camphor.[39] In detail, however, gathering structural information of larger molecules with the help of Coulomb explosion techniques faces yet multiple technical challenges. These are, for example, the initial generation of high charge states, the rapidly declining detection efficiency for the coincident detection of multiple molecular fragments,[40] and uncertainties in their correct m/q assignment. In addition, the inversion of the measured momentum-space information to position-space is far from trivial as soon as the charge-up of the molecule and/or its fragmentation is governed by nuclear dynamics. Already when examining small molecules as H_2O, support from sophisticated theory is required for the interpretation of Coulomb explosion data, which in turn provides valuable details on the fragmentation dynamics and processes.[41]

In this article, we demonstrate in a proof-of-principle study how to overcome these obstacles. With a combination of the concepts of Coulomb explosion imaging, photoelectron diffraction imaging and support from *ab initio* modelling, we developed a method for addressing isolated molecules in the gas phase to determine their structure and their handedness. Our scheme is applicable without the need for advanced laser-alignment schemes or elaborate abilities for detecting a multitude of ionic fragments in coincidence. We will show, furthermore, that our approach allows to determine even tiny details, as, for example, a slight displacement of a hydrogen atom in a methyloxirane molecule.

Experimental method

In our study, we target methyloxirane molecule and examine its ionic fragments (occurring after photoionization and subsequent Auger decay) and the angular distributions of the emitted photoelectrons. The measurements were performed employing Cold Target Recoil Ion Momentum Spectroscopy (COLTRIMS), which is a multi-coincidence momentum-imaging technique.[42,43] In brief, ions and electrons created in the interaction of single photons from the SOLEIL synchrotron with single methyloxirane molecules were guided by electric and magnetic fields onto two time- and position-sensitive microchannel-plate detectors. From the particles' positions of impact and times-of-flight the individual trajectories inside the COLTRIMS spectrometer were reconstructed in an offline analysis of the data. This information yielded the particles' momenta and accordingly all derived observables as emission directions and kinetic energies. As a coincidence measurement has been performed, relative quantities are retrieved, as well, as, for example, relative emission angles. The experimental data were recorded at the same beamtime as the data from a previous publication. Accordingly, the identical experimental setup was used and further details on the exact parameters of the COLTRIMS reaction microscope can be found there.[44] The employed photon energy of 550 eV addressed the O 1s shell of the methyloxirane molecule leading to a photoelectron energy of about 11.5 eV, and we restricted our analysis to electrons with kinetic energy of 11.5 ± 1.5 eV in order to suppress possible background. Furthermore, we employed the aforementioned photon energy as photoelectrons of this specific kinetic energy showed a large chiral response and this electron energy is amenable for accurate calculations.[44] The measurements were performed using circularly polarized light with left and right helicity. In order to cross-check the data and the analysis, the results from both helicities were compared, taking into account the corresponding symmetries. The data shown below contain both helicities added. Several fragmentation pathways occur after the oxygen–K-shell ionization of the molecule and subsequent Auger decay(s). As detailed below, we employ for our study cases where the molecule fragmented into at least three parts of which two were charged. In order to increase statistics, the data presented in this study consists of a combination of the fragmentation channels $C_3H_6O \rightarrow C_2H_3^+ + CH_2^+ + OH^0 + 2e^-$ and $C_3H_6O \rightarrow C_2H_2^+ + CH_2^+ + H_2O^0 + 2e^-$. About 3×10^6 events were recorded for both enantiomers of the molecule and both light helicities. Two other breakup channels, namely $C_3H_6O \rightarrow C_2H_3^+ + CH_3^+ + O^0$

Open Access Article. Published on 28 Okitobba 2022. Downloaded on 07/10/2025 03:30:00.
This article is licensed under a Creative Commons Attribution 3.0 Unported Licence.

+ $2e^-$ and $C_3H_6O \rightarrow C_2H_2^+ + CH_3^+ + OH^0 + 2e^-$, cannot be used because of the following reasons: It turns out that for the latter fragmentation channels the CH_3^+ group stems from the methyl group of methyloxirane. This different fragmentation dynamics manifests itself in the fact that the measured momenta of the ions define a completely different molecular coordinate system. In addition, the interference patterns for these fragmentation channels are washed out. We suspect that this is due to a weaker correlation between the measured ionic momenta and the molecular orientation at the instant of ionization due to complex fragmentation dynamics.

Theoretical method

In order to extract information on the molecular geometry from the experimental data, we performed a modelling of the electron diffraction pattern, *i.e.*, of the molecular-frame angular emission distributions of the photoelectrons. The ionization transition amplitudes for the emission of O 1s photoelectrons of the methyloxirane enantiomers were computed by using the single-center method and code[45,46] in the relaxed-core Hartree–Fock approximation, as described in our previous work on this molecule[44] (please see the ESI document of this reference for more details, as well).

The averaging of the molecular-frame photoelectron angular emission distributions over all incident directions of the ionizing light, required for the present study, was performed analytically. The average differential cross section reads:

$$\frac{\mathrm{d}\sigma(\theta,\varphi)}{\mathrm{d}\Omega} = \sum_{LM} B_{LM}\, Y^*_{LM}(\theta,\varphi)$$

with

$$B_{LM} = \frac{1}{3}\sum_{\ell m}\sum_{\ell' m'}\sum_{k} i^{\ell+\ell'}(-1)^{\ell+m'} \times \sqrt{\frac{(2\ell+1)(2\ell'+1)(2L+1)}{4\pi}} \times \begin{pmatrix} \ell & \ell' & L \\ 0 & 0 & 0 \end{pmatrix}\begin{pmatrix} \ell & \ell' & L \\ m & -m' & M \end{pmatrix} A_{\varepsilon\ell mk} A^*_{\varepsilon\ell' m' k}$$

Here, θ and φ are the photoelectron emission angles in the frame of molecular reference, Y_{LM} are spherical harmonics, and $A_{\varepsilon\ell mk}$ are the dipole transition amplitudes for the emission of the partial photoelectron waves with the angular-momentum quantum numbers ℓ and m via the absorption of a photon of polarization k, as defined in the frame of the molecule. Because of the mutual orthogonality of the Wigner rotational matrices (which transform the ionizing light of a given polarization from the laboratory to the molecular frame), the average molecular-frame photoelectron angular distribution is independent of the polarization of the ionizing light that is used in the experiment.

Results and discussion

As mentioned above, we use synchrotron light to ionize the molecule by emission of a core electron. The emerging photoelectron is diffracted by the molecular potential and serves as a messenger providing the molecular structure information in its angular emission pattern. Molecules are in most cases unstable after the emission of a core electron. Typically, at least one more additional electron is released in an Auger decay process and, subsequently, the molecule fragments into charged and neutral pieces. It turns out that the detection of the fragmentation direction (*i.e.*, the momentum vectors) of two charged fragments of a breakup of the molecule into at least three pieces is sufficient to gather the information on the spatial orientation of the molecule, which is needed for evaluating the photoelectron interference pattern. Dictated by conservation of linear momentum, the momentum vectors of three molecular fragments lie within a plane (turquoise arrows in Fig. 1A). They can be employed to form a fragment coordinate frame (X, Y, Z) in Fig. 1A, which was built as follows: $\vec{p}_{C_3H_3^+}$ ($\vec{p}_{C_2H_2^+}$, respectively) points in the direction of the Y axis, $\vec{p}_{C_2H_3^+} \times \vec{p}_{CH_2^+}$ ($\vec{p}_{C_2H_2^+} \times \vec{p}_{CH_2^+}$) in the direction of the Z axis, and $\vec{X} = \vec{Y} \times \vec{Z}$. The actual spatial orientation of the molecule within this fragment coordinate frame at the instant of photoionization remains, however, unknown. In larger systems, the fragments' emission directions are typically only loosely connected to the direction of the molecular bonds prior to the fragmentation, in particular if only few fragments are generated. Thus, the fragment frame (X, Y, Z) deduced from the ion-direction measurement and a desired molecular coordinate frame (x', y', z') linked to its structure are typically skewed by some unknown angles (R_X, R_Y, and R_Z, *i.e.*, the rotation angles with respect to the X, Y, and Z axes). In addition, the measured ion momentum vectors alone do not provide any information on the handedness of the ionized molecule, as they define a plane and thus leave the sign of the Z axis open, as depicted in Fig. 1B and C. Both, this information and the information on the skew-angles are, however, encoded in the electron diffraction pattern.

To extract the structural information from the experimental data, we use the procedure that is outlined in Fig. 2. We start with an initial guess for the molecular structure and compute the photoelectron interference pattern in a guessed molecular frame (x', y', z'), which is assumed to coincide with the fragment frame. Then, we compare this pattern to the pattern obtained in our experiment, which is provided in the fragment frame (X, Y, Z). To quantify the agreement, we introduce the distance parameter d_2 between the renormalized experimental and computed interference patterns. This parameter depends, as well, on the relative rotation between (x', y', z') and (X, Y, Z) quantified by the rotation angles R_X, R_Y, and R_Z and the guess of the handedness.

$$d_2 = \left(\iint\left(I^{\mathrm{Exp}}_{\mathrm{Norm}}(\varphi,\cos(\theta)) - I^{\mathrm{Comp}}_{\mathrm{Norm}}(\varphi,\cos(\theta),R_X,R_Y,R_Z)\right)^2 \mathrm{d}\varphi\, d\cos\theta\right)^{\frac{1}{2}}$$

We now determine the skew between the coordinate frames (x', y', z') and (X, Y, Z) varying the three rotation angles in order to obtain the smallest distance parameter d_2 (Fig. 2C). The

 This journal is © the Owner Societies 2022

Open Access Article. Published on 28 Oktobba 2022. Downloaded on 07/10/2025 03:30:00.
This article is licensed under a Creative Commons Attribution 3.0 Unported Licence.

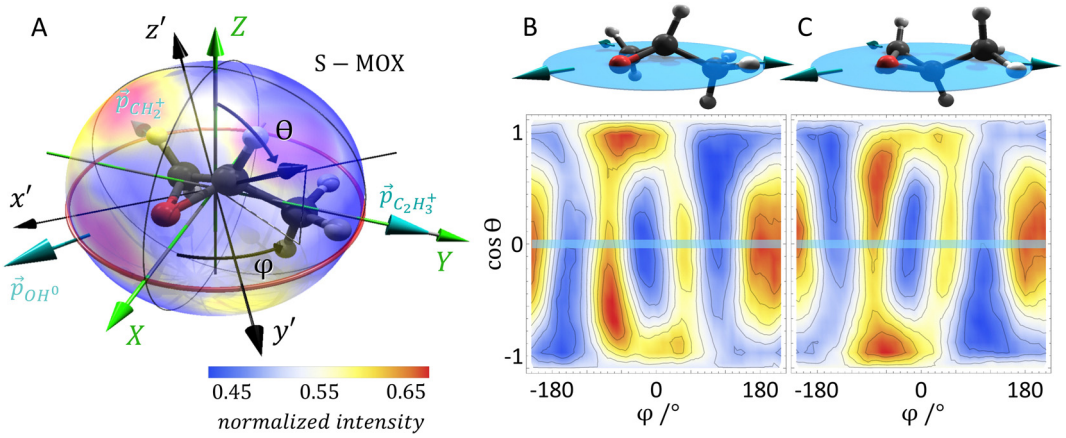

Fig. 1 Three-dimensional interference pattern of the scattered electron wave in the molecular frame of reference. **A** Spherical representation and definition of the fragment (*X*, *Y*, *Z*) and molecular (*x*′, *y*′, *z*′) coordinate frames. For larger molecules, the fragment emission directions (*i.e.*, their momenta after Coulomb explosion) do typically not coincide with molecular features such as bonds. As a result, the molecular coordinate frame (*x*′, *y*′, *z*′) at the instant of photoionization is rotated against the fragment frame (*X*, *Y*, *Z*). The panel depicts the methyloxirane molecule employed in our studies, and the turquoise arrows show the directions of the measured momentum vectors of the fragments (CH_2^+, $C_2H_3^+$, and OH^0), which were used to generate the fragment (*X*, *Y*, *Z*) coordinate system, as discussed in the text. The electron wave employed for probing the molecular structure has been emitted from the oxygen 1s orbital. The surrounding colored sphere shows the resulting three-dimensional probability distribution of the emission direction of the 11.5 eV photoelectron. The emission distributions are averaged over all incident directions of the ionizing light. **B** Same data as in **A** in a color-map representation. **C** is as **B** for the R-enantiomer. The mirror symmetry regarding the enantiomers is highlighted by the horizontal line to guide the eye at $\cos\theta = 0$ in **B** and **C**. A visualization of the two enantiomers and their orientation in the molecular frame are given above **B** and **C**.

minimized value of d_2 (*i.e.*, after applying the rotation) is then used to quantify the overall agreement between the measured and the computed interference pattern for the initially hypothesized molecular structure and handedness. This procedure is then repeated with a slightly adjusted molecular structure in terms of bond length or angles as an input in order to further minimize d_2. The model structure, which provides the smallest distance parameter d_2, is assumed to be responsible for the

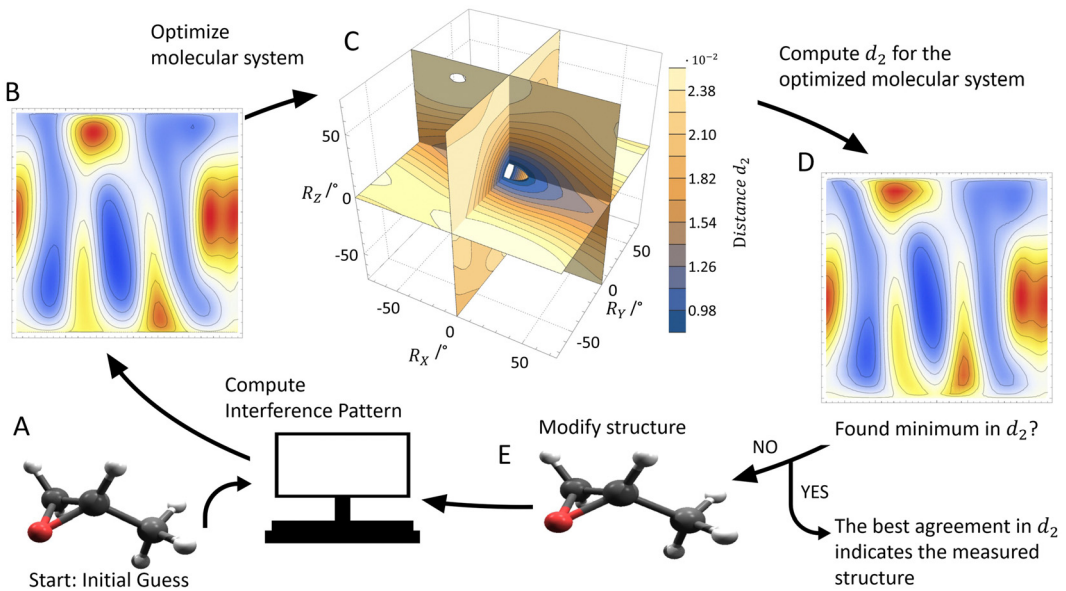

Fig. 2 Sketch of the optimization procedure for obtaining the molecular structure from the measured electron interference patterns. Starting with an initial guess (**A**) the interference pattern of the photoelectron in a chosen molecular frame (*x*′, *y*′, *z*′) is computed (**B**). This computed pattern is then compared to the measured interference pattern in the fragment frame (*X*, *Y*, *Z*). Typically, the fragment frame and molecular frame do not coincide. The skew between the two systems (given by the three rotation angles R_X, R_Y, and R_Z) is determined by finding the minimum value of the distance parameter d_2 for the computed molecular structure (**C**). **D** shows the computed interference pattern from **B** in the rotated molecular frame (*x*′, *y*′, *z*′). After the rotation, the minimized value of d_2 is used to quantify the agreement between measured and computed interference patterns for a specific hypothesized molecular structure. The molecular structure is slightly modified, and the interference pattern is recomputed (**E**). The molecular structure and coordinate system at the instant of ionization are obtained for the best agreement between measured and computed interference patterns, *i.e.*, for lowest d_2.

Open Access Article. Published on 28 Okitobba 2022. Downloaded on 07/10/2025 03:30:00.
This article is licensed under a Creative Commons Attribution 3.0 Unported Licence.

measured interference patterns, thus providing the molecular structure and coordinate system at the instant of ionization.

In more detail, in order to actually calculate the distance parameter d_2, we apply the following procedure: The minimum value occurring in the interference pattern is first subtracted from the pattern and then the pattern's integral is normalized to one. In this way, one compares two stretched two-dimensional distributions. For each calculated molecular structure, the molecular system in coordinate space used in the calculation must be connected to the measured fragment momentum vectors. To do this, we rotate the measured and calculated interference pattern with respect to each other, applying the *X*–*Y*–*Z* convention (roll, pitch, and yaw angle: R_X, R_Y, and R_Z). We determine the transformation that connects the fragment system defined by the measured ionic momenta and a molecular system used in the computation by performing a full scan of the global minimum of d_2 in the whole three-dimensional rotational space of the yaw, pitch, and roll angles (see Fig. 2C). We scan all angles in steps of one degree. This step size is small enough to ensure that the residual error in the molecular frame does not influence the result presented in the following.

In order to test our approach, we employ the two enantiomers of methyloxirane as benchmark systems. As outlined in the Experimental method section, we are using a photoelectron of 11.5 eV kinetic energy emitted from the oxygen *K*-shell for the diffraction imaging and a naturally occurring subsequent Auger decay for the generation of two ionic and one neutral fragments. As shown in Fig. 1B and C, the observed interference pattern is vastly different for the two enantiomers making chiral discrimination straightforward. A comparison to the modelled pattern shown in Fig. 2D provides the information on the absolute configuration. As the geometry of methyloxirane is well known in the literature,[47] we employ the algorithm described above (and illustrate the high sensitivity of our approach) in order to extract the exact location of distinct atoms inside the molecule. A corresponding table of the atomic coordinates at its equilibrium can be found in the ESI of ref. 44. As a first example, we show in Fig. 3A–F the effect of a modification of the CC*–O distance (*i.e.*, the distance of the oxygen atom to the CC* bond) in the oxirane ring around the equilibrium structure. The resulting variation of d_2 is shown in Fig. 3F and implies that we are sensitive to a change of 5% of the geometry-optimized CC*–O distance. For comparison, a similar relative accuracy of a few percent for a bond-length measurement has been demonstrated recently employing LIED examining OCS molecules.[48] Particularly challenging for other methods of structure determination is the assignment of the location of hydrogen atoms. Electron scattering is known to be sensitive also to such weak scatterers. Accordingly, in a second demonstration, we investigate the sensitivity of our approach to a change of the C*–H bond length. The corresponding results are depicted in Fig. 3G, which confirms that within 5% discrepancy, the correct bond length between the chiral carbon atom and the adjacent proton attached to it has been found via the smallest value of d_2.

The experimental statistical error is smaller than the plotted dot size; however, different sources of systematic errors might alter the exact value of d_2. The quality of the reconstruction as well as the achievable resolution depends on multiple factors, which cannot be easily quantified. For example, the recorded interference pattern has a finite experimental resolution. It is, however, not easy to estimate how resolving fine details of the

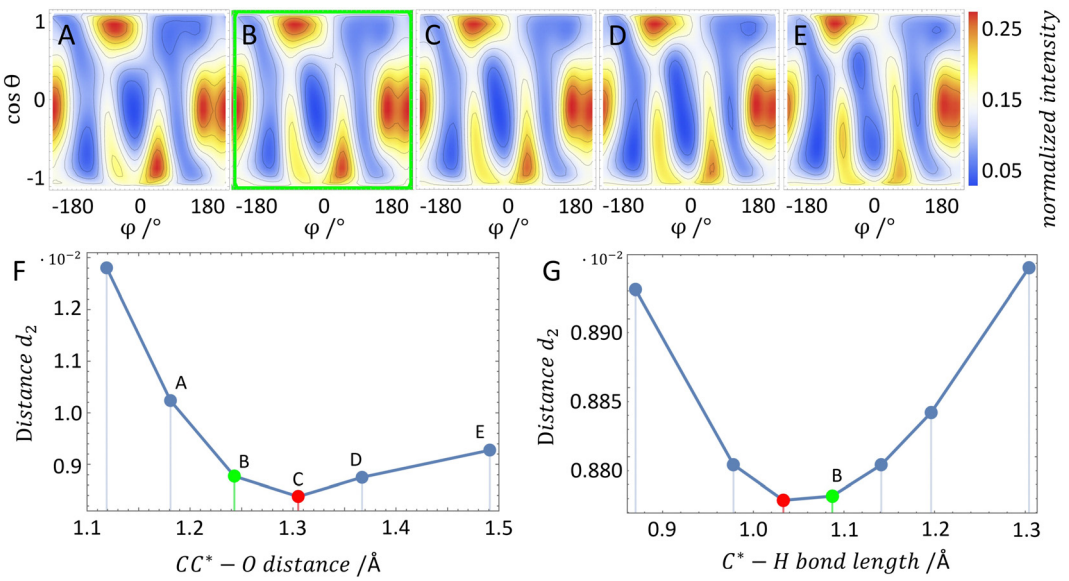

Fig. 3 Determination of the molecular structure *via* the best agreement between measured and computed interference pattern of the photoelectron. **A–E** Interference patterns from a scan in which the CC*–O distance in the oxirane ring is set to 95, 100, 105, 110, and 120% of the optimized structure. Our structure-retrieval algorithm leads within 5% accuracy to the energy-optimized structure highlighted in green (**F**). **G** A corresponding scan of the C*–H bond length demonstrates the sensitivity of the interference pattern to weak scatterers such as hydrogen. The smallest distance in d_2 leads, again, within 5% accuracy to the C*–H bond length of the energy-optimized structure.

 This journal is © the Owner Societies 2022

Open Access Article. Published on 28 Okitobba 2022. Downloaded on 07/10/2025 03:30:00.
This article is licensed under a Creative Commons Attribution 3.0 Unported Licence.

interference pattern affects the reconstruction of geometrical features in the end. First estimates on the presented data suggest that the experimental resolution is not limiting the accuracy of the geometrical reconstruction. Furthermore, background from other fragmentation channels or a complex interplay between areas of reduced detection efficiency on the electron and ion detectors might affect the geometry reconstruction, as well. Yet, we expect that the statistics of the recorded datasets has a stronger impact on the reconstruction quality in our present study. An additional source of errors is connected to the approximation that is made in the *ab initio* computations. Each molecular configuration was calculated only for fixed internuclear distances (*i.e.*, a single fixed molecular geometry) and only for a single photoelectron energy. In the experiment, however, the signal is averaged over a certain distribution of photoelectron energies and real-life molecules exhibit vibrational motion. In the case of a non-linear relationship between the influencing parameters and the observed variable, the mean value of the observed variable generally does not correspond to the mean value of the influencing factors. Therefore, an estimate of our resolution when determining the three-dimensional position of the atoms is provided by considering how close the minimum in d_2 comes to the result of the geometry-optimized structure when scanning across different molecular structures. Thus, the resolution is estimated to be of similar magnitude as our chosen step size of $\sim 6 \times 10^{-12}$ m. Please note that with our technique the spatial resolution is not limited by the photoelectron's wavelength of 3.6 Å.

Conclusion

Combining partial Coulomb explosion imaging of a large molecule with the measurement of the photoelectron diffraction pattern in the molecular frame and quantum chemical computation allows for precise structural analysis and chiral discrimination of molecules in the gas phase. Unlike established X-ray or several of the electron diffraction techniques, our approach does not require a molecular crystal. Contrary to traditional Coulomb explosion imaging, it is scalable, so that larger molecules can be examined, as well. The only requirement is that the molecule breaks sufficiently fast into at least three fragments (of which at least two are charged), so that the measured ion momentum vectors are linked to the molecular orientation at the time of ionization. In addition, by adjusting the photon energy, distinct atoms of the molecule can be addressed and the emission source of the probing electron wave inside the molecule can be selected. By applying pump–probe schemes, the method will allow for tracking changes in the molecular structure on a femtosecond time scale[49,50] in the future. The described approach is in principle general and can be extended to larger molecules. If necessary, required calculations can rely on density functional theory (DFT) based methods, which are usually not limited by molecular size, like, *e.g.* the TDDFT B-spline LCAO formalism.[51]

Data availability

All data needed to evaluate the conclusions in the paper are present in the paper. Additional data related to this paper may be requested from the authors. Correspondence and requests for materials should be addressed to K. F. (fehre@atom.uni-frankfurt.de), P. V. D. (demekhin@physik.uni-kassel.de), or M. S. S. (schoeffler@atom.uni-frankfurt.de).

Author contributions

The experiment was conceived by M. S. S. and R. D. The experiment was prepared and carried out by S. G., G. K., S. E., F. T., J. R., A. H., D. T., C. J., M. P., S. Z., F. W., M. W., M. K., M. H, L. Ph. H. S., A. K., A. H., L. B. L., A. E., R. B., H. F., K. U., T. J., J. B. W., and M. S. S. Data analysis was performed by K. F. and M. S. S. Theoretical calculations were performed by P. V. D. and N. M. N. All authors discussed the results and commented on the manuscript. K. F., P. V. D., R. D., T. J., and M. S. S. wrote the paper.

Conflicts of interest

The authors declare that they have no competing interests.

Acknowledgements

We acknowledge synchrotron SOLEIL (Saint-Aubin, France) for the provision of experimental facilities. The experiment was carried out at the beamline SEXTANTS. We thank D. Reich for discussion. We thank A. Czasch und O. Jagutzki from Roentdek GmbH for support with the detectors. We thank the staff of SOLEIL for running the facility and providing beamtimes under projects 20140056 and 20141178 and especially SEXTANTS beamline for their excellent support. This work was funded by the Deutsche Forschungsgemeinschaft (DFG) – Project No. 328961117 – SFB 1319 ELCH (Extreme light for sensing and driving molecular chirality). K. F. and A. H. acknowledge support by the German National Merit Foundation. M. S. S. thanks the Adolf-Messer Foundation for financial support. H. F. and K. U. acknowledge the XFEL Priority Strategy Program of MEXT, the Research Program of ''Dynamic Alliance for Open Innovations Bridging Human, Environment and Materials'', and the IMRAM project for support.

References

1 X. Zou and S. Hovmöller, Electron crystallography: imaging and single-crystal diffraction from powders, *Acta Crystallogr., Sect. A: Found. Crystallogr.*, 2008, **64**, 149–160.
2 D. P. Woodruff, Photoelectron diffraction: from phenomenological demonstration to practical tool, *Appl. Phys. A: Mater. Sci. Process.*, 2008, **92**, 439–445.
3 T. Kunde and B. M. Schmidt, Microcrystal Electron Diffraction (MicroED) for Small-Molecule Structure Determination, *Angew. Chem., Int. Ed.*, 2019, **58**, 666–668.

Open Access Article. Published on 28 Okitobba 2022. Downloaded on 07/10/2025 03:30:00.
This article is licensed under a Creative Commons Attribution 3.0 Unported Licence.

4 J. M. Zuo, I. Vartanyants, M. Gao, R. Zhang and L. A. Nagahara, Atomic Resolution Imaging of a Carbon Nanotube from Diffraction Intensities, *Science*, 2003, **300**, 1419–1421.
5 L. Palatinus, P. Brázda, P. Boullay, O. Perez, M. Klementová, S. Petit, V. Eigner, M. Zaarour and S. Mintova, Hydrogen positions in single nanocrystals revealed by electron diffraction, *Science*, 2017, **355**, 166–169.
6 K. Hedberg, L. Hedberg, D. S. Bethune, C. A. Brown, H. C. Dorn, R. D. Johnson and M. de Vries, Bond Lengths in Free Molecules of Buckminsterfullerene, C_{60}, from Gas-Phase Electron Diffraction, *Science*, 1991, **254**, 410–412.
7 A. A. Fokin, *et al.*, Intramolecular London Dispersion Interaction Effects on Gas-Phase and Solid-State Structures of Diamondoid Dimers, *J. Am. Chem. Soc.*, 2017, **139**, 16696–16707.
8 M. Centurion, Ultrafast imaging of isolated molecules with electron diffraction, *J. Phys. B: At., Mol. Opt. Phys.*, 2016, **49**, 062002.
9 H. N. Chapman, *et al.*, Femtosecond X-ray protein nanocrystallography, *Nature*, 2011, **470**, 73–77.
10 Y. Inokuma, S. Yoshioka, J. Ariyoshi, T. Arai, Y. Hitora, K. Takada, S. Matsunaga, K. Rissanen and M. Fujita, X-ray analysis on the nanogram to microgram scale using porous complexes, *Nature*, 2013, **495**, 461–466.
11 S. Lee, E. A. Kapustin and O. M. Yaghi, Coordinative alignment of molecules in chiral metal-organic frameworks, *Science*, 2016, **353**, 808–811.
12 T. Gruene, *et al.*, Rapid Structure Determination of Microcrystalline Molecular Compounds Using Electron Diffraction, *Angew. Chem., Int. Ed.*, 2018, **57**, 16313–16317.
13 C. J. Hensley, J. Yang and M. Centurion, Imaging of Isolated Molecules with Ultrafast Electron Pulses, *Phys. Rev. Lett.*, 2012, **109**, 133202.
14 J. Yang, *et al.*, Diffractive imaging of a rotational wavepacket in nitrogen molecules with femtosecond megaelectronvolt electron pulses, *Nat. Commun.*, 2016, **7**, 11232.
15 T. Kierspel, *et al.*, X-ray diffractive imaging of controlled gas-phase molecules: Toward imaging of dynamics in the molecular frame, *J. Chem. Phys.*, 2020, **152**, 084307.
16 C. I. Blaga, *et al.*, Imaging ultrafast molecular dynamics with laser-induced electron diffraction, *Nature*, 2012, **483**, 194–197.
17 B. Wolter, *et al.*, Ultrafast electron diffraction imaging of bond breaking in di-ionized acetylene, *Science*, 2016, **354**, 308–312.
18 A. Sanchez, *et al.*, Molecular structure retrieval directly from laboratory-frame photoelectron spectra in laser-induced electron diffraction, *Nat. Commun.*, 2021, **12**, 1520.
19 A. Landers, *et al.*, Photoelectron Diffraction Mapping: Molecules Illuminated from Within, *Phys. Rev. Lett.*, 2001, **87**, 013002.
20 H. Fukuzawa, *et al.*, Probing molecular bond-length using molecular-frame photoelectron angular distributions, *J. Chem. Phys.*, 2019, **150**, 174306.
21 M. Meckel, *et al.*, Laser-Induced Electron Tunneling and Diffraction, *Science*, 2008, **320**, 1478–1482.
22 P. Hockett, C. Z. Bisgaard, O. J. Clarkin and A. Stolow, Time-resolved imaging of purely valence-electron dynamics during a chemical reaction, *Nat. Phys.*, 2011, **7**, 612–615.
23 R. Boll, *et al.*, Femtosecond photoelectron diffraction on laser-aligned molecules: Towards time-resolved imaging of molecular structure, *Phys. Rev. A*, 2013, **88**, 061402(R).
24 J. B. Williams, *et al.*, Imaging Polyatomic Molecules in Three Dimensions Using Molecular Frame Photoelectron Angular Distributions, *Phys. Rev. Lett.*, 2012, **108**, 233002.
25 M. Yamazaki, J.-i Adachi, T. Teramoto, A. Yagishita, M. Stener and P. Decleva, 3D mapping of photoemission from a single oriented H_2O molecule, *J. Phys. B: At., Mol. Opt. Phys.*, 2009, **42**, 051001.
26 R. Fasel, J. Wider, C. Quitmann, K.-H. Ernst and T. Greber, Determination of the Absolute Chirality of Adsorbed Molecules, *Angew. Chem., Int. Ed.*, 2004, **43**, 2853–2856.
27 I. Nevo, L. Holmegaard, J. H. Nielsen, J. L. Hansen, H. Stapelfeldt, F. Filsinger, G. Meijer and J. Küpper, Laser-induced 3D alignment and orientation of quantum state-selected molecules, *Phys. Chem. Chem. Phys.*, 2009, **11**, 9912–9918.
28 K. Amini, *et al.*, Alignment, orientation, and Coulomb explosion of difluoroiodobenzene studied with the pixel imaging mass spectrometry (PImMS) camera, *J. Chem. Phys.*, 2017, **147**, 013933.
29 J. J. Larsen, K. Hald, N. Bjerre, H. Stapelfeldt and T. Seideman, Three Dimensional Alignment of Molecules Using Elliptically Polarized Laser Fields, *Phys. Rev. Lett.*, 2000, **85**, 2470.
30 J. Küpper, *et al.*, X-Ray Diffraction from Isolated and Strongly Aligned Gas-Phase Molecules with a Free-Electron Laser, *Phys. Rev. Lett.*, 2014, **112**, 083002.
31 D. Rolles, *et al.*, Femtosecond x-ray photoelectron diffraction on gas-phase dibromobenzene molecules, *J. Phys. B: At., Mol. Opt. Phys.*, 2014, **47**, 124035.
32 S. Fleischer, Y. Zhou, R. W. Field and K. A. Nelson, Molecular Orientation and Alignment by Intense Single-Cycle THz Pulses, *Phys. Rev. Lett.*, 2011, **107**, 163603.
33 Z. Vager, R. Naaman and E. P. Kanter, Coulomb Explosion Imaging of Small Molecules, *Science*, 1989, **244**, 426–431.
34 Z. Bao, R. F. Fink, O. Travnikova, D. Céolin, S. Svensson and M. N. Piancastelli, Detailed theoretical and experimental description of normal Auger decay in O_2, *J. Phys. B: At., Mol. Opt. Phys.*, 2008, **41**, 125101.
35 M. Pitzer, *et al.*, Direct Determination of Absolute Molecular Stereochemistry in Gas Phase by Coulomb Explosion Imaging, *Science*, 2013, **341**, 1096–1100.
36 K. Fehre, *et al.*, Enantioselective fragmentation of an achiral molecule in a strong laser field, *Sci. Adv.*, 2019, **5**, eaau7923.
37 M. Pitzer, *et al.*, Stereochemical configuration and selective excitation of the chiral molecule halothane, *J. Phys. B: At., Mol. Opt. Phys.*, 2016, **49**, 234001.
38 R. Boll, *et al.*, X-ray multiphoton-induced Coulomb explosion images complex single molecules, *Nat. Phys.*, 2022, **18**, 423–428.
39 C. Saribal, A. Owens, A. Yachmenev and J. Küpper, Detecting handedness of spatially oriented molecules by Coulomb explosion imaging, *J. Chem. Phys.*, 2021, **154**, 071101.

Open Access Article. Published on 28 Okitobba 2022. Downloaded on 07/10/2025 03:30:00.
This article is licensed under a Creative Commons Attribution 3.0 Unported Licence.

40 K. Fehre, *et al.*, Absolute ion detection efficiencies of microchannel plates and funnel microchannel plates for multicoincidence detection, *Rev. Sci. Instrum.*, 2018, **89**, 045112.
41 T. Jahnke, *et al.*, Inner-Shell-Ionization-Induced Femtosecond Structural Dynamics of Water Molecules Imaged at an X-Ray Free-Electron Laser, *Phys. Rev. X*, 2021, **11**, 041044.
42 J. Ullrich, R. Moshammer, A. Dorn, R. Dörner, L. Ph. H. Schmidt and H. Schmidt-Böcking, Recoil-ion and electron momentum spectroscopy: reaction-microscopes, *Rep. Prog. Phys.*, 2003, **66**, 1463.
43 T. Jahnke, Th. Weber, T. Osipov, A. L. Landers, O. Jagutzki, L. Ph. H. Schmidt, C. L. Cocke, M. H. Prior, H. Schmidt-Böcking and R. Dörner, Multicoincidence studies of photo and Auger electrons from fixed-in-space molecules using the COLTRIMS technique, *J. Electron Spectrosc. Relat. Phenom.*, 2004, **141**, 229–238.
44 M. Tia, *et al.*, Observation of Enhanced Chiral Asymmetries in the Inner-Shell Photoionization of Uniaxially Oriented Methyloxirane Enantiomers, *J. Phys. Chem. Lett.*, 2017, **8**, 2780–2786.
45 Ph. V. Demekhin, A. Ehresmann and V. L. Sukhorukov, Single center method: A computational tool for ionization and electronic excitation studies of molecules, *J. Chem. Phys.*, 2011, **134**, 024113.
46 S. A. Galitskiy, A. N. Artemyev, K. Jänkälä, B. M. Lagutin and Ph. V. Demekhin, Hartree-Fock calculation of the differential photoionization cross sections of small Li clusters, *J. Chem. Phys.*, 2015, **142**, 034306.
47 M. C. Tam, N. J. Russ and T. D. Crawford, Coupled cluster calculations of optical rotatory dispersion of (S)-methyloxirane, *J. Chem. Phys.*, 2004, **121**, 3550.
48 E. T. Karamatskos, G. Goldsztejn, S. Raabe, Ph. Stammer, T. Mullins, A. Trabattoni, R. R. Johansen, H. Stapelfeld, S. Trippel, M. J. J. Vrakking, J. Küpper and A. Rouzée, Atomic-resolution imaging of carbonyl sulfide by laser-induced electron diffraction, *J. Chem. Phys.*, 2019, **150**, 244301.
49 G. Kastirke, *et al.*, Photoelectron Diffraction Imaging of a Molecular Breakup Using an X-Ray Free-Electron Laser, *Phys. Rev. X*, 2020, **10**, 021052.
50 J. Yang, *et al.*, Simultaneous observation of nuclear and electronic dynamics by ultrafast electron diffraction, *Science*, 2020, **368**, 885–889.
51 M. Stener, G. Fronzoni and P. Decleva, Time-dependent density-functional theory for molecular photoionization with noniterative algorithm and multicenter B-spline basis set: CS_2 and C_6H_6 case studies, *J. Chem. Phys.*, 2005, **122**, 234301.